GEOPHYSICAL RESEARCH LETTERS, VOL. 27, NO. 9, PAGES 1287-1290, MAY 1, 2000

Arctic Oscillation and Arctic Sea-Ice Oscillation

Jia Wang
International Arctic Research Center-Frontier Research System for Global Change, University of Alaska Fairbanks

Moto Ikeda
Graduate School of Environmental Earth Science Hokkaido University, Sapporo, Japan

Abstract. The variability of the sea-ice cover in the Arctic and subpolar regions associated with the Arctic Oscillation (AO) was investigated using historical data from 1901 to 1997. Unrotating principal component analyses (or empirical orthogonal functions, EOFs) were applied to demeaned, normalized sea-level pressure (SLP), surface air temperature (SAT), and sea-ice area (SIA) for the periods 1901-97 and 1953-97. The leading SLP EOF mode is the AO. The leading SIA EOF mode is named the Arctic Sea-Ice Oscillation (ASIO), which accounts for 41% of the total variance for the period of 1901-1995. This dominant ASIO is AO-related; its spatial and temporal patterns are consistent with the leading modes of SLP and SAT, and with the total arctic sea-ice anomalies. The second SIA mode is North Atlantic Oscillation (NAO)-related because sea-ice anomalies in the Labrador Sea region and the Greenland Sea region are out of phase. During the last three decades, the arctic sea ice has significantly decreased, which may be the decreasing phase of long term variations.

Introduction

In previous studies of Arctic sea-ice variability [*Walsh and Johnson* 1979; *Wang et al.* 1994, 1995; *Mysak et al.* 1996; *Mysak and Venegas* 1998; Slonosky et al. 1997], the major sea-ice anomalies, obtained by using the first leading empirical orthogonal functions (EOF) modes of SLP, SAT, and sea-ice cover, were tied to the NAO [*van Loon and Rogers* 1978; *Hurrel and van Loon* 1997].

Thompson and Wallace [1998, TW98 hereafter] first proposed the idea of the AO being the dominant mode in the central Arctic, which has become increasingly evident since 1990 [*Baldwin et al.*, 1994; *Kitoh et al.* 1996; *Kodera et al.*, 1996]. *Mysak et al.* [1996] and *Walsh et al.* [1996] also observed a recent decrease in the SLP in the central Arctic since 1989. Based on the literature [TW98; *Kitoh et al.* 1996; and many others], the AO, which is associated with the polar vortex aloft, might include the NAO as a subset, depending on the domain being considered. *Mysak and Venegas* [1998, MV98 hereafter] proposed a feedback loop for the decadal climate oscillation using SLP and sea ice concentration (SIC) data from 1953-92.

In this note, we offer another new view of the AO in decadal time scales [TW98; MV98], but from both annual and seasonal views. We further propose the idea of the ASIO, using updated sea-ice data from 1901-1995 (1901-1997 for SLP and SAT) and 1953-1995. We also offer a new look at the relationships and differences between the AO and the NAO, as well as their relation to the ASIO.

Paper number 1999GL002389.
0094-8276/00/1999GL002389$05.00

Data and Methods

The monthly sea-ice concentration (SIC) data analyzed are similar to those used in Walsh and Johnson (1979) and *Wang et al.* [1995]. However, in this study, the sea-ice data that were updated using the NASA-derived SMMR (scanning multichannel microwave radiometer)/SSMI (special sensor microwave imager) sources from October 1978 were used. This dataset has been updated to August 1995 and covers the Arctic Ocean and the adjacent seas with a 1° x 1° latitude-latitude grid. Using the updated (satellite) data from 1978, *Cavalieri et al.* [1997] found a decrease in sea-ice cover in the Arctic. The monthly SLP data we used were obtained from the National Center for Atmospheric Research (NCAR) for the period of 1899-1997, archived on 5° x 5° global grids. The SAT data are from *Jones* [1994] for the period 1856-1997. The EOF analyses showed that both periods (1901-1997 and 1953-97) produce similar spatial and temporal patterns, although the data before 1953 may contain some uncertainty.

Following *Wang et al.* [1995], the Arctic Ocean is divided into eight regions: 1) the Bering Sea, 2) the Beaufort and Chukchi Seas, 3) Hudson Bay, 4) Baffin Bay/Davis Strait and the Labrador Sea, 5) the Greenland and Norwegian Seas, 6) the Barents and Kara Seas, 7) the East Siberian and Laptev Seas, and 8) the Sea of Okhotsk.

AO and ASIO: A Seasonal View of Decadal Time Scales

The first leading EOF modes for SLP, SAT, and SIA were obtained from the monthly anomaly fields north of 45°N for the period 1901-1997 (Figs. 1-3, upper panels) with the corresponding annual (Figs. 1-3, middle) and seasonal time series of coefficients (Figs. 1-3, lower). The spatial SLP pattern is typical of results obtained by *Wang et al.* [1995], *Mysak et al.* [1996, see their Fig. 16], TW98 [see their Fig. 2], and MV98. The annual time series of the coefficients (Fig. 1, middle) indicates a drastic decrease since 1989 [*Wang et al.* 1995; *Walsh et al.* 1996; TW98]. However, the seasonal time series of the leading EOF mode (Fig. 1, lower) indicate that the winter SLP anomaly has the largest amplitude (variance or variation, see also Table 1). The summer SLP anomaly is comparable to the spring and autumn anomalies. In 1989, the SLP for all seasons decreased (negative anomalies), indicating that the AO encompasses all four seasons compared with the winter-prevailing NAO. To verify the consistency between this study and TW98, we calculated the correlation coefficients of the 5-year running means between the AO index [TW98] and our first SLP mode (r=0.54) and between the NAO index and our first SLP mode (r=0.42). Note that the differences between TW98 and this study are 1) we used monthly data, while TW98 used winter month mean data, and 2) our domain is north of 45°N, while TW98 used nearly northern hemispheric data (north of 20°N).

The leading SAT mode (Fig. 2, upper) shows a warming in most arctic regions, except for the Labrador Sea where cooling is observed. Strongest warming occurs in Europe, while moderate warming is located in northwestern America and slight warming occurs in the other regions, such as the Bering Sea, Gulf of Alaska, and central Arctic. *Slonosky et al.* [1997] also showed a warming in the central Arctic from the 850-mb temperature (see their Fig. 9). A small warming in the North Pacific sector implies that the local climate is also coupled to another dominating player, such as the North Pacific Oscillation that is associated with the Southern Oscillation [*Minobe* 1997]. The annual time series of the leading SAT mode (Fig. 2, middle) indicates decadal variability embedded with a small warming trend since the beginning of this century. Since 1970s, the arctic region has experienced three strong warming events: 1970s, 80s, and 90s. The 1990s event was the strongest and the longest, and it is this Arctic warming that we have been monitoring and discussing worldwide. A seasonal view of the three warming events since 1970s, particularly the recent 1990s warming, indicates that the arctic warming events took place persistently throughout four seasons (Fig. 2, lower). For example, since 1989, all four seasons experienced warming, with winter and spring temperatures showing the most increase (also see Table 1).

The leading SIA mode (Fig. 3, upper) clearly demonstrates an in-phase fluctuation in all eight regions: up or down (i.e., increase or decrease in SIA). Thus, we define the Arctic Sea-Ice Oscillation (ASIO) as the in-phase fluctuation in the Arctic SIA anomalies and its annual and seasonal indices as its leading EOF coefficients (Fig. 3, middle and lower). This new finding differs from that of *Mysak et al.* [1996] who showed that the leading SIA mode is the NAO-related mode. The reason for the difference is that their study was based on the SIC data only from 1953 to 1990, and those data originated from conventional observations. The data used in this note have been updated using satellite data since August 1978. The annual time series (Fig. 3, middle) shows variability on both decadal and even longer (century) time scales. Note that the SIA has decreased since 1972, particularly in 1978, which may be due to the transition from conventional observations to satellite-observed data. Thus, this dataset contains some uncertainty in the mean value, due to the possible systematic error caused by the different measurement means. However, the tendency of anomalous variability will not be affected. A new finding is that the ASIO (Fig. 3, lower) is greatest in summer, rather than in winter (and other seasons), even though the winter SAT anomaly (Fig. 2, lower) is the greatest (see also Table 1). The common feature, compared with SAT anomalies, is that the ASIO has four-season persistency, which is not likely explained by the NAO that only dominates in winter season. Therefore, the summer SIA anomaly contributes the most to the annual anomaly. It should be pointed out that the SIA anomaly has occurred since 1972, particularly in the last two decades; however, this does not mean a "linear trend" with respect to the mean of the nearly 100-year time series. The argument of the linear trend may be valid only if the data since 1970s are considered. The decrease in SIA since 1972 may be due to natural climate

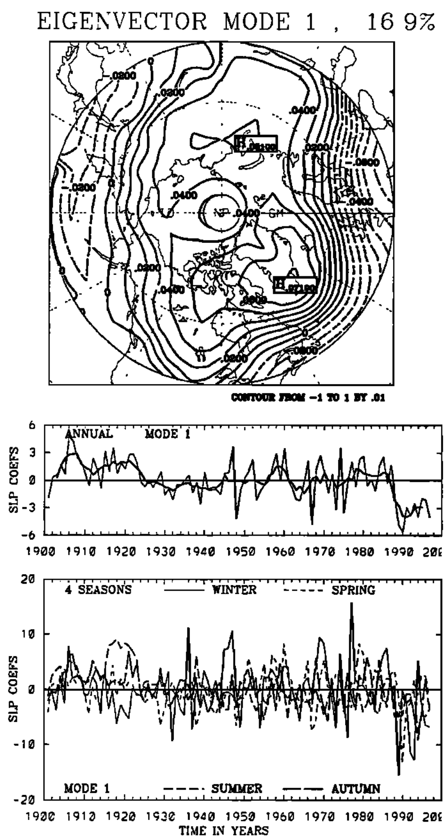

Figure 1. The eigenvectors (spatial pattern) for the leading SLP EOF mode (AO, upper panel), the time series of the annual coefficient (middle) with a 5-year running mean (thick line) and the four seasonal coefficients (lower). The spatial and temporal patterns of the anomalies of the (AO) mode can be reconstructed by multiplying the coefficients to the eigenvectors.

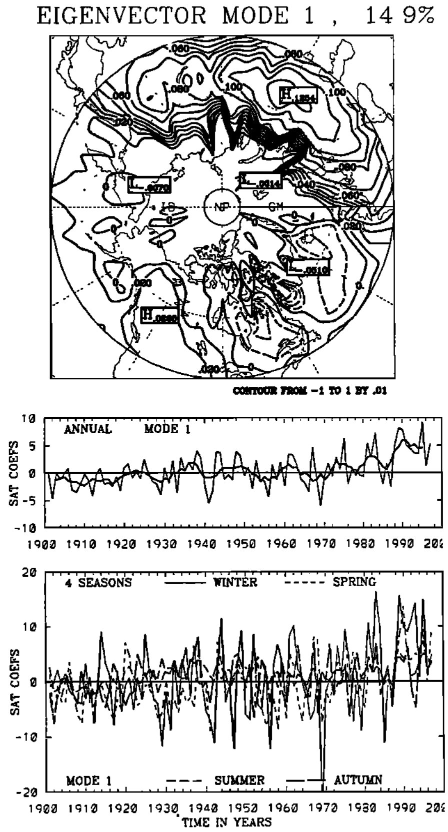

Figure 2. Same as Fig. 1, except for SAT anomalies.

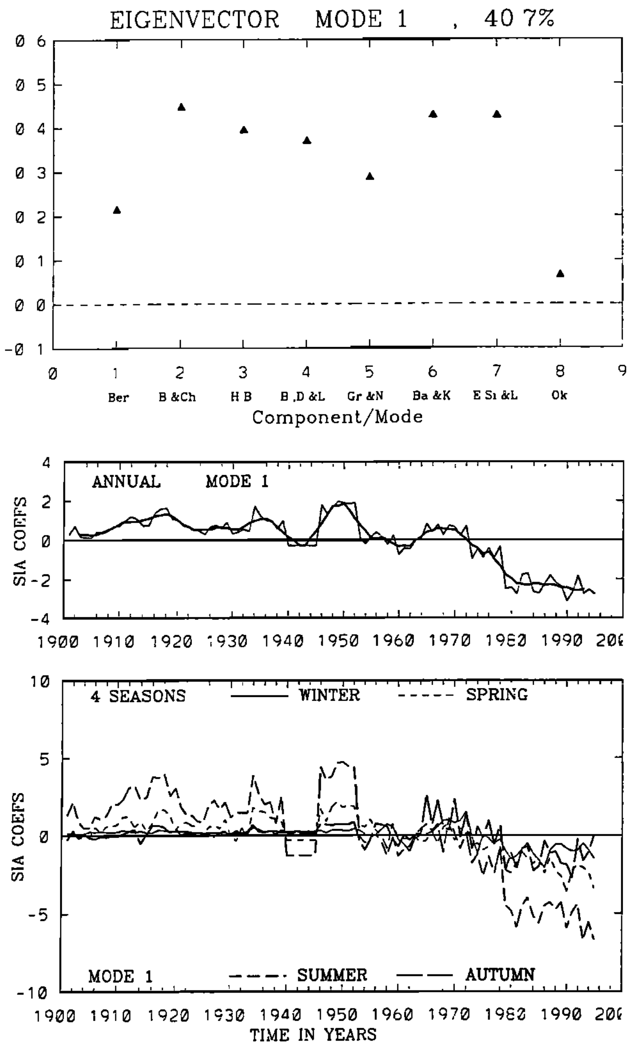

Figure 3. Same as Fig. 1, except for SIA anomalies (i.e., ASIO).

variability with longer (century) time scales, while the present climate is speculated to be at the trough of the climate variability.

To confirm the leading role of the ASIO, we calculated the time series of the annual and four-season SIA anomalies (Fig. 4), which mimic the time series of the first SIA EOF mode (i.e., ASIO, Figs. 3, middle and lower), at a level of r=0.99. Again, the greatest standard deviation of the sea-ice data also occurs in summer (Table 1). The total SIA deduction from 1972 to 1995 is about 1.2×10^6 km^2, i.e., 5×10^4 km^2 per year, which is consistent with the thinning of the Arctic sea-ice cover [*Rothrock et al.* 1999].

To further support the argument for the AO [TW98; MV98] and the ASIO, we performed a Monte Carlo simulation [*Wang et al.* 1994] of the SLP, SAT, and SIA anomalies over nearly 100-year data. We only discuss the correlation over 95% significance level in the following. The leading SLP mode (AO) correlates to SAT over all four seasons (Table 2, upper pair), indicating that the AO operates slightly differently from the NAO, whose index correlates to SAT anomaly only in three seasons: winter, spring, and autumn [see the fourth row of Table 2 of *Mysak et al.* 1996]. Furthermore, the leading SAT mode (associated with the AO) correlates to the leading SIA mode (i.e., ASIO) over all four seasons (Table 2, middle pair), while NAO-related SAT correlates to the SIA

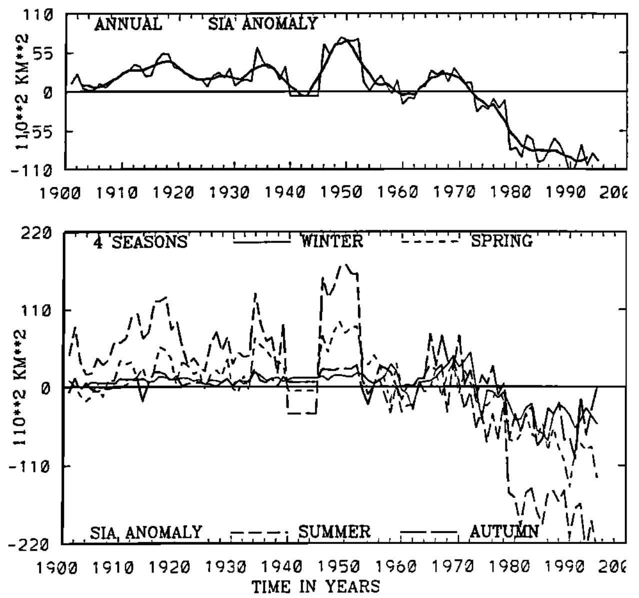

Figure 4. Same as Fig. 3 (middle and lower), except for the observed total arctic SIA anomalies.

anomaly only in winter and autumn [see the third row of Table 1 of *Mysak et al.* 1996]. We also calculated the correlation between the first SAT mode (AO-related) and the second SIA mode; the correlation over the 95% significance level occurs only in winter (r=-0.31; i.e., NAO-related).

The significant correlation between the summer SLP and SIA (Table 2, lower pair) occurs only in spring (r=0.33) and summer (r=0.29). This implies that wind driving (by an AO-related SLP anomaly) of the SIA through convergence and divergence is most effective in spring and summer when there exits open waters. Therefore, the wind stress anomaly certainly results in sea-ice thickness redistribution and sea-ice flux out of the Arctic Ocean [*Proshutinsky and Johnson* 1997; Kw*ok and Rothrock* 1999].

Conclusion and Discussion

1) Accompanying and in response to the AO (in terms of SLP), the ASIO is found in response to the AO-related SAT anomaly over all four seasons (thermodynamic link), distinguished from the NAO, which prevails in winter, spring, and autumn, and weakens in summer [see the fourth row of Table 2 of *Mysak et al.* 1996; *Barnston and Livezey* 1987; *Rogers* 1990]. The AO-related wind forcing on the arctic SIA is most effective in spring and summer (dynamic link), rather than in winter and autumn, resulting in redistribution of sea-ice thickness.

Table 1. Standard deviations (STDs) of time series of the first leading modes of SLP, SAT, SIA, and the total Arctic sea-ice anomaly. The maximum STDs are boldfaced.

STDs	Winter	Spring	Summer	Autumn	Annual
SLP (Mode 1)	**5.04**	3.44	3.37	3.51	2.17
SAT (Mode 1)	**6.79**	4.88	1.86	3.51	3.08
SIA (Mode 1)	0.62	1.24	**2.93**	0.89	1.31
SIA (Data)	24.48	47.76	**99.70**	30.50	46.89

Table 2. Simultaneous and lagged correlation coefficients (r, with 95% significance levels derived from a Monte Carlo simulation) between the leading annual SLP and SAT modes (upper pair; 1901-1997), between the leading annual SAT and SIA (ASIO) modes (middle pair; 1901-1995), and between the leading summer SLP and SIA (ASIO) modes (lower pair; 1901-1995). The coefficients over 95% significance level are boldfaced.

Statistics	Winter	Spring	Summer	Autumn	Annual
Annual SLP and SAT (Mode 1)					
r	**-0.44**	**-0.46**	**-0.50**	**-0.40**	**-0.64**
95% S.L.	0.25	0.25	0.25	0.25	0.25
Annual SAT and SIA (Mode 1)					
r	**-0.37**	**-0.44**	**-0.44**	**-0.33**	**-0.46**
95% S.L.	0.27	0.26	0.26	0.26	0.27
Summer SLP and SIA (Mode 1)					
r	0.14	**0.33**	**0.29**	0.16	**0.28**
95% S.L.	0.25	0.26	0.28	0.25	0.26

2) Even though the largest SAT anomaly occurs in winter, the summer SIA anomaly contributes most to the annual anomaly (Tables 1 and 2), implying air-ice-sea interactions (i.e., a feedback system) at work [MV98; *Steele and Boyd* 1998; *McPhee et al.* 1998; *Ikeda et al.* 2000].

3) The difference between the AO and the NAO is that the AO operates seasonwide and correlates to the SAT, also seasonwide, producing a persistent pattern, while the NAO (index) correlates to SAT anomalies only in winter (strongest), spring, and autumn, but not summer. The SAT mode 1 coefficients correlate to the SIA mode 1 coefficients in all four seasons, while the NAO-related SAT anomaly correlates to SIA anomaly only in winter and autumn. Thus, the NAO may be considered as a subset of the AO if the study region is focused in the Arctic [TW98; also *Wallace*, personal comm.].

4) The leading (AO) modes of SLP, SAT, and SIA all capture the drastic change since 1989. In the past decade, arctic SLP/SAT/SIA have experienced a decrease/increase /decrease tendency. However, this does not mean linear trends exist for these climate variables. Based on nearly 100 years of data, we speculate that the present climate warming scenario in the Arctic is the combination of a natural oscillation of longer time scales and the steadily increasing greenhouse gases released by anthropogenic activities.

Acknowledgements. We thank the Frontier Research System for Global Change, through JAMSTEC, Japan for financial support. We thank two anonymous reviewers for their constructive comments on this contribution. The authors appreciate fruitful discussions with M. Wallace, D. Thompson, L. Mysak, J. Walsh, K. Aagaard, M. Steele, R. Gerdes, and S. Minobe.

References

Baldwin, M.P., X. Cheng, and T.J. Dunkerton, 1994. Observed correlation between winter-mean tropospheric and stratospheric circulation anomalies. *Geophys. Res. Lett., 21*, 1141-1144.

Barnston, A.G. and R.E. Livezey, 1987. Classification, seasonality and persistence of low-frequency atmospheric circulation patterns. *Mon. Wea. Rev, 115*, 1083-1126.

Cavalieri, D.J., P. Gloersen, C.L. Parkinson, J.C. Comiso, and H.J. Zwally, 1997. Observed hemispheric asymmetry in global sea ice changes. *Science, 278*, 1104-1106.

Hurrell, J.W. and H. van Loon, 1997. Decadal variations in climate associated with the North Atlantic Oscillation. *Climate Change, 36*, 301-326.

Kitoh, A. H. Koide, K. Kodera, S. Yukimoto, and A. Noda, 1996. Interannual variability in the stratospheric-tropospheric circulation in a coupled ocean-atmosphere GCM. *Geophys. Res. Lett, 23*, 543-546.

Kodera, K., M. Chiba, H. Koide, A. Kitoh, and Y. Nikaidou, 1996. Interannual variability of the winter stratosphere and troposphere in the Northern Hemisphere. *J. Meteorol. Soc. Japan, 74*, 365-382.

Ikeda, M., J. Wang and J.-P. Zhao, 2000. Hypersensitive decadal oscillation in the Arctic/subarctic climate (submitted to *GRL*).

Jones, P.D., 1994. Hemispheric surface air temperature variations: A reanalysis and update to 1993. J. Climate, 7, 1794-1802.

Kwok, R. and D.A. Rothrock, 1999 Variability of Fram Strait ice flux and North Atlantic Oscillation. *J. Geophys. Res., 104*. 5177-5189.

McPhee, M.G., T.P. Stanton, J.H. Morison, and D.G. Martinson, 1998. Freshening of the upper ocean in the Arctic: is perennial sea ice disappearing? *Geophys. Res. Lett., 25*, 1729-1732.

Minobe, S., 1997. A 50-70 year climate oscillation over the North Pacific and North America. *Geophys. Res. Lett, 24*, 683-686.

Mysak, L.A. and S.A. Venegas, 1998. Decadal climate oscillations in the Arctic: a new feedback loop for atmosphere-ice-ocean interactions. *Geophys. Res. Lett, 25*, 3607-3610.

Mysak, L.A., R.G. Ingram, J. Wang, and A. van der Baaren, 1996. The anomalous sea-ice extent in Hudson Bay, Baffin Bay and the Labrador Sea during three simultaneous NAO and ENSO episodes. *Atmosphere-Ocean, 34*, 314-343.

Proshutinsky, A.Y. and M.A. Johnson, 1997. Two circulation regimes of the wind-driven Arctic Ocean. *J. Geophys Res., 102*, 12,493-12,514.

Rogers, J.C., 1990. Patterns of low-frequency monthly sea level pressure variability (1899-1986) and associated wave cyclone frequencies. *J. Climate, 3*, 1364-1379.

Rothrock, D.A., Y. Yu, and G.A. Maykut, 1999. Thinning of the Arctic sea-ice cover. *Geophys. Res. Lett., 26*, 3469-3472.

Slonosky, C.S., L.A. Mysak, and J. Derome, 1997. Linking arctic sea-ice and atmospheric circulation anomalies on interannual and decadal time scales. *Atmosphere-Ocean, 35*, 333-366.

Steele, M. and T. Boyd, 1998. Retreat of the cold halocline layer in the Arctic Ocean. *J. Geophys. Res., 103*, 10,419-10,435.

Thompson, D.W.J. and J.M. Wallace, 1998. The Arctic Oscillation signature in the wintertime geopotential height and temperature fields. *Geophys Res. Lett, 25*, 1297-1300.

Van Loon, H. and J.C. Rogers, 1978. The seesaw in winter temperature between Greenland and northern Europe, Part 1: General description. *Mon. Wea. Rev., 106*, 296-310.

Walsh, J.E. and C.M. Johnson, 1979. Interannual atmospheric variability and associated fluctuations in Arctic sea ice extent. *J. Geophys. Res. 84*, 6915-6928.

Walsh, J.E., W.L. Chapman, and T.L. Shy, 1996. Recent decrease of sea level pressure in the central Arctic. *J. Climate, 9*, 480-486.

Wang, J., L.A. Mysak, and R.G. Ingram, 1994. Interannual variability of sea-ice cover in Hudson Bay, Baffin Bay and the Labrador Sea. *Atmosphere-Ocean, 32*, 421-447.

Wang, J., A. van der Baaren, and L.A. Mysak, 1995. A principal component analysis of gridded sea-level pressure, surface air temperature, and sea-ice concentration of the arctic region, 1953-1993. C2GCR Rep. No. 95-4, McGill Univ., 18pp + figures +Fortran programs. (available at the International Arctic Research Center, University of Alaska Fairbanks: jwang@iarc.uaf.edu)

J. Wang, International Arctic Research Center-Frontier Research System for Global Change, University of Alaska Fairbanks, Fairbanks, Alaska 99775-7335 (e-mail: jwang@iarc.uaf.edu)

M. Ikeda, Graduate School of Environmental Earth Science Hokkaido University, Sapporo, Japan (e-mail: mikeda@ees.hokudai.ac.jp)

(Received August 1999; revised December 1999; accepted January 2000.)